Application of positron annihilation and Raman spectroscopies to the study of perovskite type materials

D. Grebennikov,[1,a)] O. Ovchar,[2,b)] A. Belous,[2,c)] and P. Mascher[1,d)]
[1]*Department of Engineering Physics and Centre for Emerging Device Technologies, McMaster University, Hamilton, Ontario L8S 4L7, Canada*
[2]*V. I. Vernadskii Institute of General and Inorganic Chemistry NAS of Ukraine, 32/24 Palladin Ave., 03680 Kyiv-142, Ukraine*

(Received 31 August 2010; accepted 14 October 2010; published online 10 December 2010)

Defect properties of perovskite type materials, $Ba_3B'Nb_2O_9$ (where B′=Mg, Zn, or Co), with near-stoichiometric compositions were studied by positron annihilation and Raman spectroscopies. Theoretical simulations of stoichiometric perovskites revealed a dependence of the positron bulk lifetime on the degree of ordering. In $Ba_3MgNb_2O_9$ (BMN) the positron bulk lifetime for a completely disordered structure is 195 ps versus 237 ps for a completely ordered one. The predicted bulk lifetimes for $Ba_3ZnNb_2O_9$ (BZN) and $Ba_3CoNb_2O_9$ (BCN), with $Pm\bar{3}m$ symmetries are 193 ps and 194 ps, respectively. It was found that deviation from stoichiometry results in the appearance of secondary Ba- and Nb-rich phases, which according to theoretical simulations have bulk lifetimes much longer than that of the host material. Positron lifetime spectroscopy was used to monitor changes in the concentration of these second phases. The difference between predicted defect lifetimes and the bulk values for the studied perovskites was less than 70 ps. This and the likely small concentrations made it impossible to discern the presence of point defects in the samples. Raman measurements demonstrated the presence of a particular mode that could be attributed to the formation of a 1:1 phase, the size of which is limited by requirements for charge compensation. The existence of an internal electric field between charged 1:1 nanoregions and the rest of material creates conditions for preferential positron annihilation that influence the obtained positron lifetime values. For BZN type materials it was found that the degree of 1:2 cation ordering decreases by increasing the sintering temperature to above 1400 °C. © *2010 American Institute of Physics*. [doi:10.1063/1.3517098]

I. INTRODUCTION

Rapid growth of wireless technologies over the last decade has significantly stimulated research on new materials suitable for dielectric resonator applications. Perovskite oxides based on the formula $Ba(B'_{1/3}B''_{2/3})O_3$, where B′=Mg, Zn, or Co and B″=Ta or Nb, are materials known to possess high dielectric constants and low losses. Recent research on perovskite type materials as dielectric resonators was concentrated mostly on Nb-based compounds since high sintering temperatures (1600–1650 °C) and long soaking times (~50 h) made Ta-based perovskites commercially unattractive.

$Ba(B'_{1/3}Nb_{2/3})O_3$ (B′=Mg, Zn, or Co) perovskites represent order-disorder type materials. When disordered they have cubic unit cells with $a_0 \approx 0.409$ nm depending on the ionic size of B′ cations and can be described in the $Pm\bar{3}m$ space group. The 1:2 ordered compounds adopt a trigonal symmetry having the $P\bar{3}m1$ space group due to the distortion along the ⟨111⟩ direction of the cubic cell. The value of unit cell distortion, that is usually characterized by $c/a > \sqrt{3}/2$, where c and a are the sizes of, respectively, hexagonal ordered and cubic disordered unit cells, depends on the size and charge difference between two cations on the B-site. It is well established that B-site cation ordering has significant influence on dielectric losses at microwave frequencies.[1,2] The ordering process involves cation "swapping" between two identical crystallographic sites. The presence of point defects can significantly enhance the ordering process. The role of defects in the transition between two phases can be either to provide vacant sites for the neighboring B-site cation to exchange its position or to distort the cation environment thereby changing the lattice repulsive potential.[3] In addition to influencing cation ordering the introduction of point defects in the crystal lattice can result in the formation of additional crystal phases having structures different from the main material.[4]

In the present study the effect on the 1:2 ordering of Ba and B′-site deficiency in complex perovskites $Ba(B'_{1/3}Nb_{2/3})O_3$ (where B′=Mg, Zn, or Co) with near-stoichiometric compositions was investigated by means of positron annihilation and Raman spectroscopies.

Literature results for the application of Raman spectroscopy to perovskite type materials are quite contradictory and mode assignment is mostly based on the correlation between changes in position and line shapes of the bands and expected changes in the ordering degree. Kim *et al.*[5] studied $Ba(Ni_{1/3}Nb_{2/3})O_3$ and $Ba(Zn_{1/3}Nb_{2/3})O_3$ systems and found a

a)Electronic mail: grebend@mcmaster.ca.
b)Electronic mail: ovcharoleg@yahoo.com.
c)Electronic mail: belous@ionc.kar.net.
d)Electronic mail: mascher@mcmaster.ca.

connection between the appearance of certain Raman peaks and x-ray diffraction (XRD) lines arising from the presence of ordered domains. Siny *et al.*[6] considered the coexistence of 1:1 and 1:2 B-site cation ordering in complex perovskites. The starting point was that the completely disordered $Pm\bar{3}m$ phase is not Raman active. Partial 1:1 cation ordering is expected to produce four Raman modes, and according to group theoretical analysis, long-range 1:2 ordering often observed in Ba-based complex perovskites should give rise to nine Raman active modes. Formation of 1:1 ordered domains in perovskites containing 1:2 composition of B-type cations will require charge compensation by the rest of the material. The requirements to compensate for charge imbalance inside of 1:1 ordered regions restrict their growth and make commonly used crystallographic techniques such as XRD insensitive to their presence. Generally, Raman modes of $Ba(B'_{1/3}B''_{2/3})O_3$ (B′=Mg, Zn, or Co and B″=Ta or Nb) perovskites all are similar in shape and close in band position.[2,7–9]

Positron annihilation spectroscopy proves to be highly sensitive to the change in the electronic environment caused by impurities having electronic densities different from those of the host material and to the presence of different kinds of defects. In solids positrons can annihilate after thermalization either from the delocalized bulk state with the characteristic bulk lifetime (τ_b) or be localized in and annihilate from one of the defect states that are characterized by the defect lifetime (τ_d). The bulk lifetime is determined by the average electron density of the material, that is, by the electronic configuration of constituent atoms and the lattice parameters of material. The presence of defects with reduced electron density such as point defects, open volumes, and grain boundaries can significantly increase the time that a positron exists in solids. The rate of positron trapping in vacancy defects k_d depends on the defects' concentration and results in reduction in the experimentally observed bulk lifetime (the so-called reduced bulk lifetime τ_1). In practice, limited resolution of the equipment used for positron lifetime measurements results in that only one or two defect lifetimes can be observed. In the case of the presence of only one type of defect and not all implanted positrons annihilating at defect sites, the one defect trapping model is used to extract the experimentally observed bulk lifetime[10]

$$\tau_b = \left(\frac{I_1}{\tau_1} + \frac{I_2}{\tau_2}\right)^{-1}. \quad (1)$$

Here I_1 and I_2 are the probabilities of a positron to be annihilating from, respectively, the delocalized bulk or localized defect states and τ_1 and τ_2 are the reduced bulk and defect lifetimes.

There are a limited number of publications involving studies of positron annihilation in perovskite type materials. In 2000, Ghosh and Nielsen theoretically predicted bulk and defect lifetimes for several ABO_3 perovskite structures ($LaCoO_3$, $BaTiO_3$, and $PbTiO_3$) having only one type of cation on the B-sublattice.[11] In their simulations they, assuming cubic symmetry of the considered structures, used the atomic superposition method,[12,13] which resulted in the following values: τ_b=129 ps for $LaCoO_3$ and ~150 ps for $BaTiO_3$ and $PbTiO_3$ materials. Introduction of defects on the A-position produces defect lifetimes ranging from 275 to 293 ps. The presence of defects on the B-sublattice would give much shorter lifetime values: from 173 ps for $LaCoO_3$ to 204 ps for $PbTiO_3$ perovskites. Experimental lifetime measurements demonstrated good correlation with calculated bulk values: 138 ps for $LaCoO_3$ (Ref. 14) versus 160 ps for $BaTiO_3$.[15] Predicted lifetimes in case of oxygen defects were close to the bulk values indicating an inability of positrons to distinguish positively charged oxygen vacancies inside of the studied materials. The biggest difference between τ_b and the positron lifetime in oxygen defects was predicted for the $LaCoO_3$ system (τ_b=129 ps versus τ_O=145 ps). This was associated with the possible change in the charge state of oxygen vacancies from positive to neutral. This was confirmed experimentally.[11] Several groups calculated bulk and defect lifetimes in $SrTiO_3$ material having cubic structure.[16,17] Mackie *et al.*[17] used atomic superposition and linear muffin-tin orbital methods with Boronski–Nieminen (BN) (Ref. 18) and Arponen–Pajanne (AP) (Ref. 19) enhancement factors. According to their simulations both methods used to approximate electron densities resulted in differences of bulk and defect lifetimes of less than 10%. The biggest difference in calculated values was observed due to different approximations used to describe the enhancement factor. In particular, calculated bulk lifetime values change from 119 to 151 ps, respectively, for BN and AP enhancement factors. Keeble *et al.*[20] considered $PbTiO_3$ and partially substituted $Pb(Zr_{0.4}Ti_{0.6})O_3$ perovskite type materials, both having tetragonal symmetry. Theoretical calculations based on the atomic superposition method with AP enhancement factor lead to bulk lifetime values of 150 ps for $PbTiO_3$ and 160 ps for $Pb(Zr_{0.4}Ti_{0.6})O_3$ systems. Formation of point defects on cation or anion sites in $PbTiO_3$ perovskites is expected to produce defect lifetimes close to those reported by Ghosh *et al.*[11] in the same system while in $Pb(Zr_{0.4}Ti_{0.6})O_3$ structures the predicted defect lifetime values are slightly longer. Based on the theoretically predicted defect lifetime values, Keeble *et al.*[20] observed formation of lead vacancies in both $PbTiO_3$ and $Pb(Zr_{0.4}Ti_{0.6})O_3$ oxides and B-site (B=Zr and/or Ti) vacancies in $Pb(Zr_{0.4}Ti_{0.6})O_3$ system.

Although the perovskites considered in the present research have the same structure as those previously reported,[11,17] substitution of different A- and B-site cations in ABO_3 perovskites with different ionic radii will result in different unit cell sizes. Changes in unit cell parameters influence the electron density and hence the positron bulk lifetime. This made us to perform our own theoretical calculations of positron lifetimes in $Ba(B'_{1/3}Nb_{2/3})O_3$ perovskites (B′=Mg, Zn, or Co) by taking advantage of the MIKA package obtained from Helsinki University of Technology.[21]

II. EXPERIMENTAL PROCEDURE

Ceramic materials were produced by a two-step mixed-oxide route. At first, columbite type materials $A_{1+x}Nb_2O_6$ (A=Mg, Zn, or Co) were synthesized. Then an appropriate ratio of $BaCO_3$ was added to the respective columbites. Ma-

TABLE I. Experimental unit cell parameters and theoretically calculated bulk and defect lifetimes

Material	$Ba_3MgNb_2O_9$	$Ba_3MgNb_2O_9$	$Ba_3CoNb_2O_9$	$Ba_3ZnNb_2O_9$
Space group	$Pm\bar{3}m$	$P\bar{3}m1$	$Pm\bar{3}m$	$Pm\bar{3}m$
Lattice parameters (Å)	$a=4.0855$	$a=5.7871$, $c=7.0674$	$a=4.0886$	$a=4.0699$
τ_b (ps)	195	237	194	193
τ_{Ba} (ps)	321		322	321
τ_B (ps)	264		264	260
τ_{Nb} (ps)	265		265	262
τ_O (ps)	197		195	194

terials were uniaxially pressed into cylindrical disks of 5–7 mm diameter and 2–4 mm height. Sintering was performed for 8 h in air at temperatures of 1350–1500 °C. Crystal lattice parameters were analyzed by XRD on a DRON—3M (Burevestnik, Russia) diffractometer with Cu K_α-radiation.

The defect structure of the studied perovskites was examined by positron lifetime spectroscopy. Each experimental spectrum contained six million counts and at least three spectra were recorded for each pair of samples. The source strength was 20 μCi and the system resolution was 280 ps. PATFIT88 was used to analyze experimental spectra.[22] After source correction (155 and 256 ps with intensities 28% and 72%, respectively, and total intensity of 9.6%) and background subtraction the spectra were decomposed into two components. The fitting procedure was monitored by chi-squared values. The average chi-squared value did not exceed 1.12. Any attempt to separate additional components in the measured spectra close to theoretically predicted values resulted in increases in χ^2 or unphysical (e.g., negative) intensity values. Based on the presence of only one defect type, the one defect trapping model was used to calculate experimental bulk lifetimes.

Raman spectra were taken at room temperature on a Renishaw2000 spectrometer, with the 514 nm line of an Ar^+ ion laser used as the excitation source. Prior to measurements the surface of samples was polished with diamond paste (9, 3, and 1 μm).

III. METHOD OF CALCULATIONS

Based on the results of XRD, the structures of materials considered in the present research were solved in terms of mixtures of a disordered phase having $Pm\bar{3}m$ space group and an ordered hexagonal phase with $P\bar{3}m1$ space group. In addition, some nonstoichiometric materials contained Ba- and Nb-rich phases. Experimentally obtained lattice parameters of the main phases (see Table I) were used to construct $4\times4\times4$ supercells containing more than 300 atoms each. The positron lifetime, defined as

$$\tau^{-1} = \pi r_0 c \int g(0,n_+,n_-)n_-(r)n_+(r)dr, \quad (2)$$

where r_0 and c are the classical electron radius and the speed of light, n_- and n_+ are electron and positron densities and g is the enhancement factor, respectively, were calculated for the bulk and for various point defects by using the atomic superposition method implemented in the MIKA package.[21] A generalized gradient approximation taking into account inhomogeneous electron distribution with parameterisation suggested by Arponen and Pajanne[19] was used to describe the enhancement of the electron density near the positron site.

IV. RESULTS AND DISCUSSION

A. $Ba_3MgNb_2O_9$ (BMN) perovskites

The transition of $Ba(B'_{1/3}Nb_{2/3})O_3$ (B′=Mg, Zn, or Co) perovskites from a disordered to a 1:2 ordered state is accompanied by a distortion of the cubic unit cell along the ⟨111⟩ direction. A change in lattice parameters caused by mutual repulsion of two small highly charged transition metal cations (Nb^{5+}) is expected to change the unit cell volume while maintaining the same number of atoms, that is, the disorder—1:2 order phase transition leads to changes in the average electron density and hence, positron bulk lifetime. Among the studied perovskites it is easier to achieve a higher degree of ordering in the $Ba_3MgNb_2O_9$ (BMN) composition because of the large ionic radius difference between magnesium and niobium. The tendency of cobalt and zinc materials for ordering is lower. So, reliable identification of 1:2 ordered structures was performed only in BMN samples. Lattice parameters of $Ba(B'_{1/3}Nb_{2/3})O_3$ (B′=Mg, Zn, or Co) perovskites as well as calculated bulk and defect lifetimes are presented in Table I. Vacancy lifetimes are indicated by the missing atom, i.e., τ_O is the lifetime of positrons annihilating in an oxygen vacancy.

Stoichiometric BMN samples were sintered at 1400 °C for 8 h. Figure 1 shows the measured XRD pattern. The

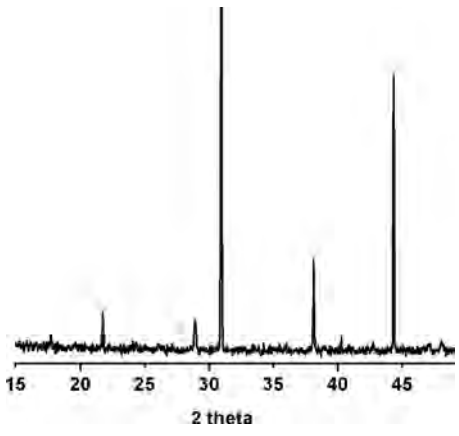

FIG. 1. X-ray spectrum of $Ba_3MgNb_2O_9$ perovskite.

TABLE II. Experimentally observed positron lifetimes and intensities for stoichiometric $Ba(B'_{1/3}Nb_{2/3})O_3$ perovskites.

	$Ba_3MgNb_2O_9$	$Ba_3CoNb_2O_9$	$Ba_3ZnNb_2O_9$
τ_1 (ps)	178 ± 1	164 ± 1	204 ± 2
τ_2 (ps)	336 ± 5	294 ± 5	355 ± 7
I_1 (%)	75 ± 2	71 ± 2	74 ± 2
I_2 (%)	25 ± 1	29 ± 1	26 ± 2

formation of the 1:2 ordered phase is characterized by an appearance of weak superlattice peaks at small diffraction angles, the strongest of which is at $2\theta = 17.7°$. Subsequent analysis demonstrates the presence of 8% of the ordered phase, with the rest of the material in the disordered state. Those results are in agreement with findings of Janaswamy[23] who studied the change in the ordering of $Ba(Mg_{1/3}B''_{2/3})O_3$ (B''=Nb or Ta) perovskites at different sintering temperatures.

According to our simulations the introduction of Ba-vacancies in the disordered phase will give a defect lifetime of 320 ps. The presence of Mg and Nb vacancies will result in a 264 ps lifetime component. From the experiment we observe the so-called "reduced" bulk lifetime component and a component arising from the annihilation in defects. Typical values of the reduced and defect lifetimes as well as their relative intensities for stoichiometric compositions of $Ba(B'_{1/3}Nb_{2/3})O_3$ oxides (B'=Mg, Zn, or Co) are presented in Table II. The studied materials consist of grains having intergranular spaces. Grain boundaries represent regions in samples with reduced electron density. We attribute the latter component, with intensities of 24%–40% for different stoichiometric and nonstoichiometric $Ba(B'_{1/3}Nb_{2/3})O_3$ perovskites (B'=Mg, Zn, or Co) and lifetime values around 300 ps, to positrons annihilating inside of intergranular spaces. Variations in the values of the defect lifetimes and their probabilities can be related to the difference in the ceramics' microstructure. We were unable to separate any additional components in the experimental lifetime spectra, which probably indicates that either the concentration of the point defects is so small that it is beyond the sensitivity of the setup used in the present studies or the resolution of the experimental setup is not sufficient to separate closely spaced components. This fact validates the application of the one defect trapping model.

The discussion above shows that changes in the symmetry significantly affect the positron results. A mixture of roughly 8% of ordered phase with the rest disordered should give an "average" value of 200 ps. This value is very close to the experimentally observed lifetime of 202 ps. Kolodiazhnyi *et al.*[24] reported $\tau_b = 205$ ps for the BMN system which is close to the value obtained in the present studies and can actually represent a mixture of two lifetimes with different values. In the absence of any additional phase it is possible to use the bulk lifetime to estimate the ordering degree in the studied perovskites.

B. $Ba_{3+3x}CoNb_2O_9$ perovskites

Stoichiometric and nonstoichiometric barium cobalt niobate samples (with varying Ba concentration $x = -0.02, -0.01, -0.005, 0, 0.005$) were sintered at 1450 °C for 8 h. The results of XRD and positron lifetime measurements are presented in Figs. 2(a) and 2(b), respectively.

According to the measured XRD patterns, the stoichiometric composition represents single-phase material. Introduction of Ba deficiencies in $Ba_{3+3x}CoNb_2O_9$ perovskites (negative x) results at first in the appearance of 1:2 order that disappears with further reduction in barium concentration and formation of an additional crystal phase [Fig. 2(a)] that corresponds to $Ba_6CoNb_9O_{30}$. The concentration of this phase increases with decrease in barium content.

Figure 2(b) shows that the bulk lifetime smoothly decreases from 204 for $x = -0.02$ to 190 ps for $x = 0.005$. The change in the bulk lifetime of barium deficient cobalt samples can be the result of the formation of the Nb-rich $Ba_6CoNb_9O_{30}$ phase. In order to check the validity of our assumptions we performed calculations of the bulk lifetime in the $Ba_6CoNb_9O_{30}$ structure. Lattice cell parameters and symmetry of the considered oxide used to construct the periodical potential were adapted from the work of Lehmann and Mueller-Buschbaum.[25] Our simulations resulted in a

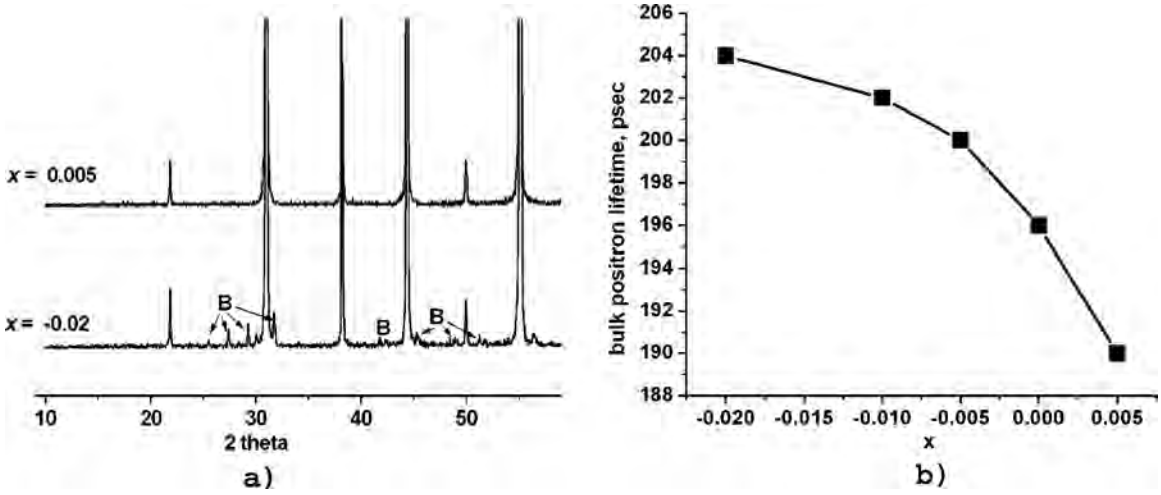

FIG. 2. (a) X-ray and (b) positron data for $Ba_{3+3x}CoNb_2O_9$ perovskites (B–$Ba_6CoNb_9O_{30}$).

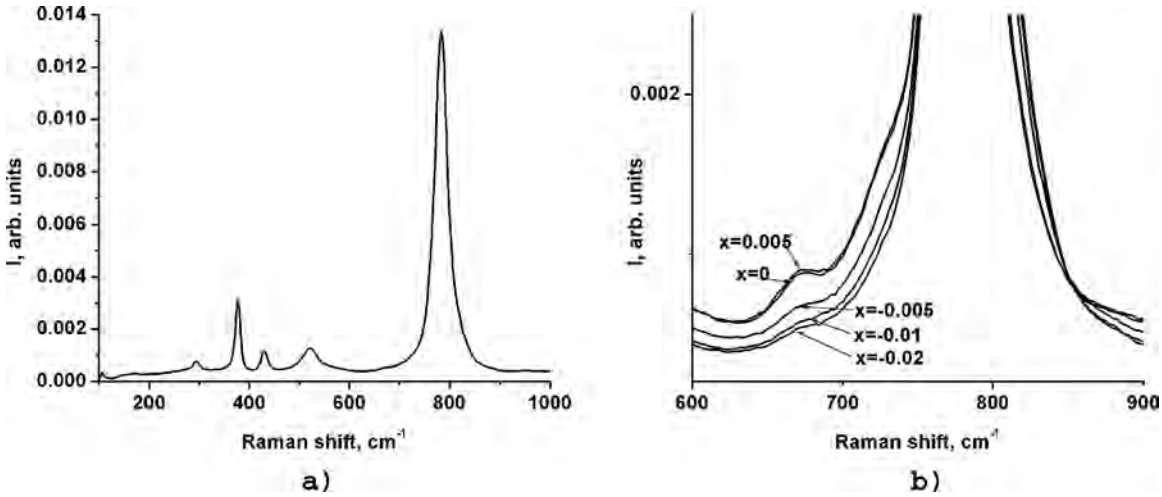

FIG. 3. (a) Typical Raman spectrum of $Ba_{3+3x}CoNb_2O_9$ perovskites and (b) formation of 1:1 ordered phase.

bulk lifetime of 353 ps for $Ba_6CoNb_9O_{30}$ material. So, the bulk lifetime in $Ba_{3+3x}CoNb_2O_9$ materials is influenced by the presence of the $Ba_6CoNb_9O_{30}$ crystal phase with much longer lifetime value (353 versus 194 for the host material, see Table I) and 1:2 ordered domains with a bulk lifetime close to that of BMN system (237 ps). By moving toward positive x values the amount of the Ba-rich phase as well as the degree of 1:2 ordering decreases [Fig. 2(a)], which is accompanied by a reduction in τ_b [Fig. 2(b)]. For $x=0$ and 0.005, τ_b is slightly shorter than the theoretically predicted bulk lifetime for the completely disordered $Ba_6CoNb_9O_{30}$ (BCN) perovskite indicating disappearance of additional phases. τ_b for the Ba-rich phase is much longer than that for the 1:2 ordered BCN perovskite. So, the reduction in the bulk lifetime arises mostly from changes in the concentration of $Ba_6CoNb_9O_{30}$.

The sensitivity of the x-ray technique to the presence of 1:2 order depends on the difference in the atomic scattering factors of B-site cations. In $Ba_3B'Nb_2O_9$ (B′=Zn or Co) systems having generally low tendency for ordering because of the small size and charge differences between B-site cations, the difference in the atomic scattering factors is small. So, subtle changes in the ordering degree could well be missed by the XRD technique. A number of publications demonstrated an application of Raman spectroscopy to detect variations in 1:2 ordering. For example, Lee *et al.*[26] studied evolution of Raman spectra in the $Ba_3ZnNb_2O_9$ (BZN) system under different preparation conditions. Dai *et al.*[27] performing theoretical calculations assigned commonly observed Raman modes in barium perovskites with 1:2 B-site cation ratio to the appearance of 1:2 ordering.

Spectra obtained in the present work are similar to those published for example for BMN and $Ba_3MgTa_2O_9$ (BMT) (Ref. 28) and BZN (Ref. 29) perovskites. The main features of the obtained spectra are formation of seven sharp modes that according to Dai *et al.*[27] are $A_{1g}(Ba)+E_g(Ba)$ at 105 cm^{-1}, $E_g(O)$ at 174 cm^{-1}, $A_{1g}(Nb)$ at 262 cm^{-1}, $E_g(Nb)$ at 295 cm^{-1}, $E_g(O)$ at 385 cm^{-1}, $A_{1g}(O)$ at 435 cm^{-1}, and $A_{1g}(O)$ at 785 cm^{-1}. The last mode is due to the collective motion of oxygen atoms forming octahedra around B-type cations. In the case of BCN perovskites where according to x-ray measurements the degree of 1:2 ordering is smaller, Raman modes become less sharp and have a tendency to smear out, confirming the validity of the mode assignment [Fig. 3(a)]. An interesting feature of the measured Raman spectra of BCN perovskites with Ba nonstoichiometry is the appearance of additional modes at 670 cm^{-1}, the intensity of which depends on the amount of nonstoichiometry: by decreasing the Ba content, the intensity of the 670 cm^{-1} mode decreases [Fig. 3(b)]. In Ref. 30, we attributed this mode to collective movement of oxygen octahedra in the 1:1 B-site ordered phase. The 1:1 ordered structure represents ordered cation arrangement in 1:1 sequence along the ⟨111⟩ direction of the perovskite cubic cell and is commonly found in $A(B'_{1/3}B''_{2/3})O_3$ perovskites containing 1:2 ratio of the B-site cations with lead on the A-site.[31,32]

Formation of 1:1 order in materials having 1:2 B-site cation ratio can be explained based on either the so-called "random-site" or "space-charge" models.[32] The random-site model considers that one of two B-sites is occupied exclusively by B″ cations, with the second B-site occupied by a random mixture of B′ and the remaining B″ cations. In this model the ordered 1:1 structure can be represented as $A[(B'_{2/3}B''_{1/3})_{0.5}B''_{0.5}]O_3$. In this case the average composition of the ordered regions is the same as that in the bulk and charge compensation is achieved within several unit cells.

According to the space-charge model, a 1:1 mixture of B′ and B″ type cations occupies the B-site while the rest of the B″ ions form regions rich in B″-cations, in order to preserve $A(B'_{1/3}B''_{2/3})O_3$ stoichiometry. This model is characterized by formation of ordered domains with deficiency of B″-type cations and nearby regions that have an excess of B″-type cations with respect to the average $A(B'_{1/3}B''_{2/3})O_3$ composition. Cation imbalance creates net negative charge within ordered domains and net positive charge in B″-rich regions. A shift in the 670 cm^{-1} mode to lower values (in comparison to its counterpart in 1:2 ordered materials) is due to the weakening of oxygen octahedra caused by an uncompensated charge inside of 1:1 ordered domains. In addition to changes in B–O bond strength, formation of excess negative charge inside of 1:1 nanoregions would create strong electric

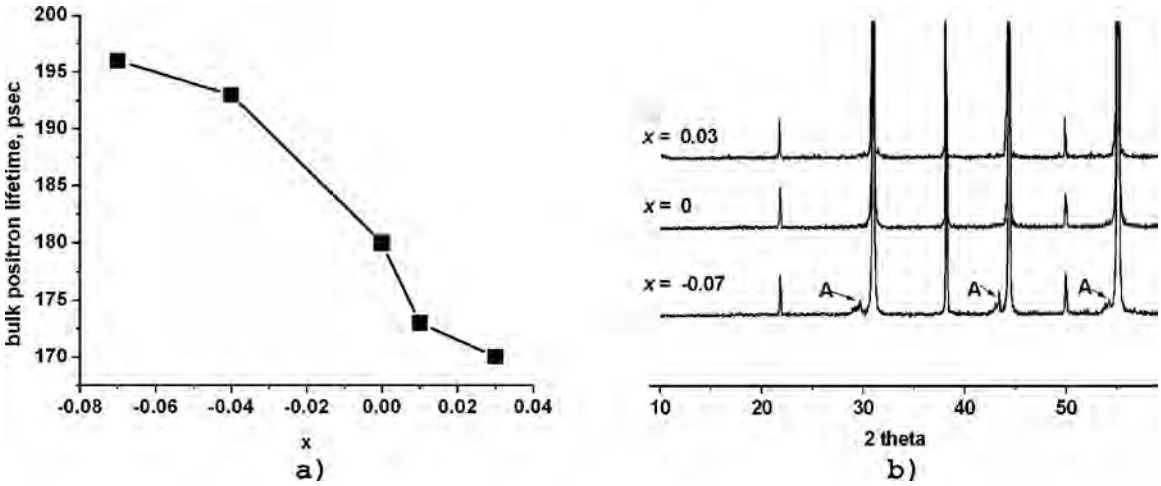

FIG. 4. (a) Bulk positron lifetime and (b) x-ray data for $Ba_3Co_{1+x}Nb_2O_9$ perovskites (A–$Ba_5Nb_4O_{15}$).

fields between ordered domains and the rest of the material. Wang *et al.*[33] observed changes in the positron migration characteristics in AlGaN/GaN heterostructures caused by the presence of a strong intrinsic electric field in the AlGaN layer that tends to move positrons from the heterointerface toward the surface of AlGaN. Internal fields between the 1:1 ordered domains and regions rich in the B″-cations can create conditions for the preferential annihilation of positrons in parts of the sample containing the 1:1 ordered domains. The presence of an excess of small B″-cations with high electron density increases the average electron density, in comparison to the main composition, at the interface between the 1:1 ordered domains and B″-rich regions decreasing positron bulk lifetime.

By looking again at Fig. 2(b) ($x=0$ and 0.005), where according to Raman results (Fig. 3) small traces of 1:2 ordering are present and the amount of 1:1 ordered phase is a maximum, the positron bulk lifetime drops below the value expected for the completely disordered phase ($\tau_b=194$ ps). This could be an indication of preferential annihilation of positrons at the interface between the 1:1 ordered domains and B″-rich regions.

C. $Ba_3Co_{1+x}Nb_2O_9$ perovskites

Positron lifetimes [Fig. 4(a)] for $Ba_3Co_{1+x}Nb_2O_9$ sintered at 1450–1500 °C for 8 h are again, influenced by changes in 1:2 ordering and concentration of additional crystal phases.

According to XRD measurements, deviation from stoichiometry on the cobalt sublattice at first promotes 1:2 ordering (for small values of x) but further decrease in cobalt content reduces the amount of 1:2 ordering and produces an additional phase. The XRD peaks of this phase could be attributed to $Ba_5Nb_4O_{15}$ that has the structure of $A_nB_{n-1}O_{3n}$ slab perovskite.[34] Structural data for the theoretical simulations of the positron bulk lifetime in the $Ba_5Nb_4O_{15}$ system were taken from the work of Pagola *et al.*[35] The predicted bulk lifetime is 426 ps. In the case of cobalt nonstoichiometries the positron behavior becomes more complex. At almost all cobalt concentrations the experimental positron bulk lifetimes are below the values predicted for the disordered system ($\tau_b=194$ ps, Table I). For the samples with barium nonstoichiometries it was found that the decrease in τ_b below the lowest theoretically predicted value is due to the presence

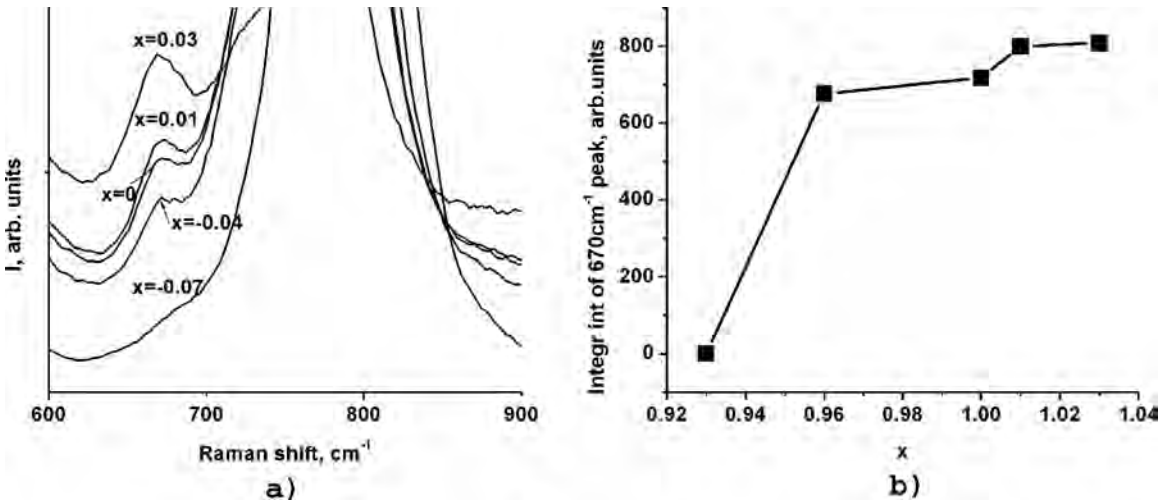

FIG. 5. (a) Magnified part of $A_{1g}(O)$ Raman mode of $Ba_3Co_{1+x}Nb_2O_9$ perovskites and (b) Integrated intensity of 670 cm^{-1} mode vs x value.

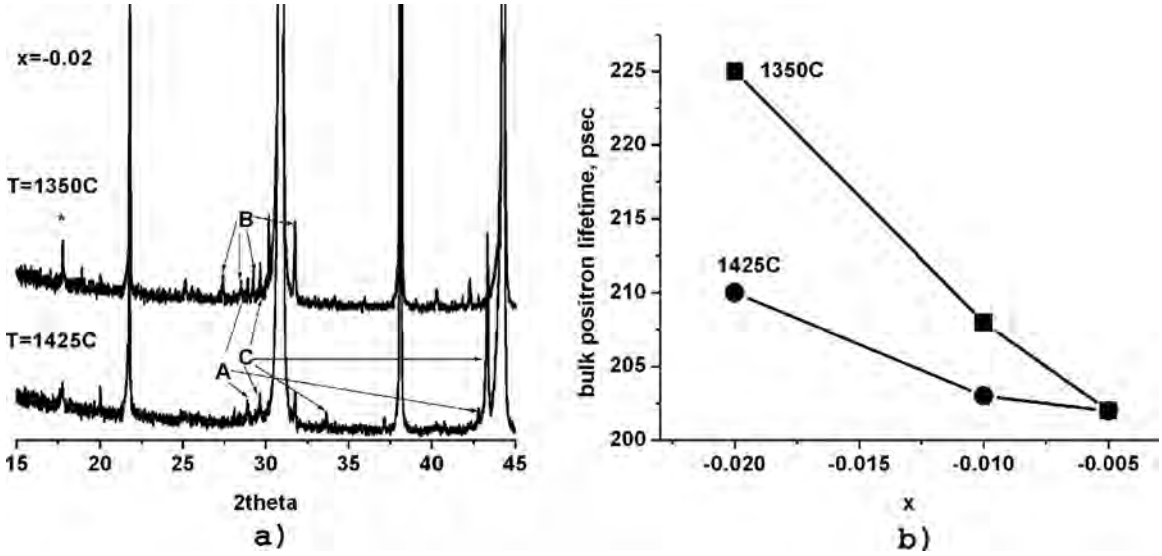

FIG. 6. (a) X-ray and (b) positron results for $Ba_{3+3x}ZnNb_2O_9$ perovskites.

of 1:1 ordered nanoregions. Figure 5(a) shows a magnified part of the $A_{1g}(O)$ Raman mode of $Ba_3Co_{1+x}Nb_2O_9$ perovskites. For cobalt nonstoichiometries the intensity of the 670 cm^{-1} band is larger indicating a larger degree of 1:1 ordering. A partially ordered phase, according to Raman results, forms at all values of x. Figure 5(b) shows the integrated intensity of the partially ordered 1:1 phase that has a maximum value in samples with excess of cobalt and decreases with the reduction in cobalt concentration. The 1:1 ordered phase demonstrates a behavior opposite to the 1:2 ordered phase: increase in the amount of one of them reduces the amount of other. Barber *et al.*[36] observed changes in the concentration of both types of ordering in $Ba_3ZnNb_2O_9$ and BMT) perovskites and noticed similar trends. The difference in the concentration of 1:1 ordered domains in the cobalt system with barium and cobalt nonstoichiometries could be explained by different lattice distortions caused by A- and B-site cation vacancies and slightly different preparation conditions used.

D. $Ba_{3+3x}ZnNb_2O_9$ versus $Ba_3Zn_{1+x}Nb_2O_9$ perovskites

Nonstoichiometric BZN samples with variations in Ba concentration were sintered at two different temperatures: 1350 and 1425 °C for 8 h. XRD [Fig. 6(a)] showed the presence of several crystal phases that were identified as analogs of $Ba_6CoNb_9O_{30}$ (found in BCN samples) and Ba-rich phases ($Ba_8ZnNb_6O_{24}$ and $Ba_5Nb_4O_{15}$) for the BZN samples sintered at lower and higher temperatures, respectively. By increasing the sintering temperature the x-ray peak indicating the presence of 1:2 ordering decreases. This is in agreement with the results of Kim *et al.*[5] who reported a structural phase transition from the ordered to the disordered phase around 1400 °C.

Theoretical simulations of bulk lifetimes in completely disordered barium zinc niobate perovskite yielded 193 ps (Table I). In the case of a 1:2 ordered system the expected τ_b should be around 240 ps as was predicted for BMN perovskite. Figure 6(b) shows positron results for the studied BZN system. Within all studied x-values the bulk lifetime is above the value for the disordered BZN perovskite and for the stoichiometric materials, approaching values of 200 ps. The crystal structure of the $Ba_8CoNb_6O_{24}$ phase, an analog to the zinc system, was reported by Mallinson *et al.*[37] as consisting of the corner sharing BO_6 octahedrons with the ordered arrangement of Co, Nb, and cation vacancies. The bulk lifetime for $Ba_8ZnNb_6O_{24}$ found in high temperature-sintered ceramics is expected to be much longer than that of the main material due to the presence of the layer containing the B-site cation vacancies that reduce the average electron density.

Again, the main factor influencing the behavior of τ_b in $Ba_{3+3x}ZnNb_2O_9$ is the change in the concentration of second phases with lifetimes much longer than that of the disordered phase forming the main part of the studied materials. Volatility of ZnO during the preparation process is likely to produce Zn-deficient $Ba_8ZnNb_6O_{24}$ and $Ba_5Nb_4O_{15}$ phases even in the samples with nominal composition. Unfortunately, the presence of several structures including 1:2 ordered domains with long lifetime values did not allow us to discern the influence of each of them on the measured τ_b.

Results of positron lifetime measurements for BZN perovskites sintered at 1450–1500 °C for 8 h with deviation from stoichiometry on the B′ subblattice are shown in Fig. 7. X-ray data revealed formation of one additional phase: $Ba_8ZnNb_6O_{24}$. No evidence of superstructure peaks was found.

By varying Zn stoichiometry τ_b smoothly decreases from 213 ps for $x=-0.07$ to almost 200 ps for stoichiometric composition. This again traces the change in the concentration of the additional phase. Contrary to the cobalt system, the bulk lifetime of zinc containing BZN perovskites does not drop below the value for the disordered phase (193 ps). Examination of Raman spectra of BZN samples did not show any evidence of 670 cm^{-1} mode formation. This is possibly due to ZnO evaporation during sintering that produced zinc deficient phases.

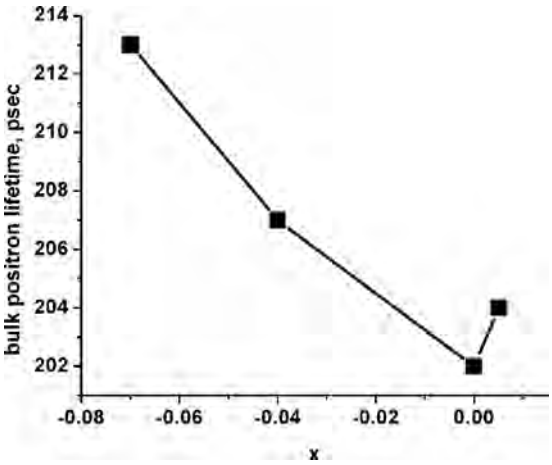

FIG. 7. Dependence of τ_b on x in $Ba_3Zn_{1+x}Nb_2O_9$ perovskites.

Finally, we compare results of theoretical simulations of the positron bulk lifetime in $Ba(B'_{1/3}Nb_{2/3})O_3$ (B′=Mg, Zn, or Co) oxides with those previously reported.[11,16,20] The considered materials have the general formula ABO_3. The crystal structure of this class of oxides is formed through corner sharing arrangement of BO_6 octahedra. The stability of the cubic ABO_3 structure is defined by geometrical compatibility of A–O and B–O bond lengths. Substitution of different types of cations with different electronic configurations and ionic radii results in structural distortion and lowering in symmetry from cubic to orthorhombic, rhombohedral, tetragonal, monoclinic, and triclinic.[38] Change in lattice parameters due to either lowering in symmetry or presence of cations with different ionic radii changes the unit cell volume and hence, the positron annihilation rate.

In Fig. 8, we show bulk lifetimes of previously reported perovskite oxides[11,16,20] as well as those obtained in the present research versus unit cell volumes used by corresponding authors for lifetime calculations. As one can see from the graph, increases in the unit cell size defined by the ionic radius of the A-site cation lead to increases in the bulk lifetime values indicating changes in the average electron density.

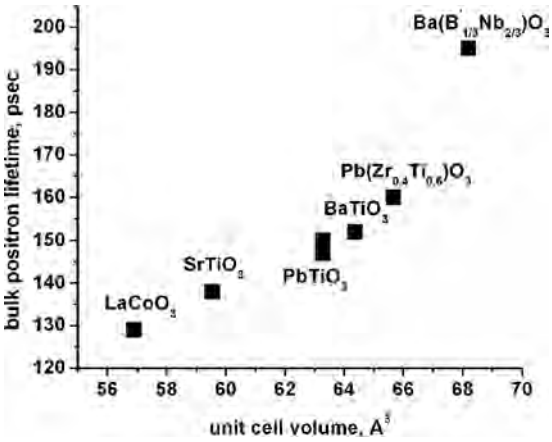

FIG. 8. Dependence of τ_b on unit cell volume for different ABO_3 perovskites.

V. CONCLUSIONS

Several stoichiometric and nonstoichiometric perovskite type materials were studied by positron annihilation and Raman spectroscopies. In spite of its sensitivity to the presence of defects in different kinds of materials, positron lifetime measurements turned out to be sensitive mainly to intercrystallite boundaries and did not find formation of any point defects. The theoretically predicted bulk lifetime for the completely disordered $Ba(B'_{1/3}Nb_{2/3})O_3$ (B′=Mg, Zn, or Co) system was found to be around 190 ps. 1:2 ordering results in an increase in τ_b to around 237 ps. Deviation from stoichiometry in the studied perovskites led to the formation of Ba, Nb-rich crystal phases with bulk lifetimes much longer than corresponding values of the matrix (353 and 423 ps, respectively for $Ba_6CoNb_9O_{30}$ and $Ba_5Nb_4O_{15}$ materials). The value of the bulk lifetime was sensitive to changes in the concentration of additional phases with variation in stoichiometry on Ba and B′-sublattices and can be used to trace variations in the ordering degree in samples without "extra" crystal phases.

Formation of partially ordered 1:1 nanoregions in cobalt systems modified positron lifetime spectra producing bulk lifetimes below theoretically predicted values. Loss of zinc oxide during the preparation process produced zinc deficient structures that possibly prevented formation of 1:1 ordered domains. All observed bulk lifetime values for BZN perovskites are above expected values indicating formation of additional phases that were not detected by XRD.

ACKNOWLEDGMENTS

This work was supported by a NATO grant under the NATO SfP Project No. 980881: "Dielectric Resonators" of the NATO "Science for Peace" Program and by the Natural Sciences and Engineering Research Council of Canada. The authors wish to thank Dr. T. Kolodiazhnyi for providing samples for Raman measurements.

[1]P. K. Davis, J. Tong, and T. Negas, J. Am. Ceram. Soc. **80**, 1724 (1997).
[2]I. T. Kim, Y. H. Kim, and S. J. Chung, Jpn. J. Appl. Phys., Part 1 **34**, 4096 (1995).
[3]W. D. Kingery, *Introduction to Ceramics* (Wiley, New York, 1976).
[4]P. K. Davies, A. Borisevich, and M. Thirumal, J. Eur. Ceram. Soc. **23**, 2461 (2003).
[5]B.-K. Kim, H.-O. Hamaguchi, I.-T. Kim, and K. S. Hong, J. Am. Ceram. Soc. **78**, 3117 (1995).
[6]I. G. Siny, T. Ruiwu, R. S. Katiyar, R. Guo, and A. S. Bhalla, J. Phys. Chem. Solids **59**, 181 (1998).
[7]H. Tamura, D. A. Sagala, and K. Wakino, Jpn. J. Appl. Phys., Part 1 **25**, 787 (1986).
[8]D. A. Sagala and S. J. Koyasu, J. Am. Ceram. Soc. **76**, 2433 (1993).
[9]M. Sugiyama and T. Nagai, Jpn. J. Appl. Phys., Part 1 **32**, 4360 (1993).
[10]R. Krause-Rehberg and H. S. Leipner, *Positron Annihilation in Semiconductors* (Springer, Berlin, 1999).
[11]V. J. Ghosh, B. Nielsen, and T. Friessnegg, Phys. Rev. B **61**, 207 (2000).
[12]V. J. Ghosh, M. Alatalo, P. Asoka-Kumar, K. G. Lynn, and A. C. Kruseman, Appl. Surf. Sci. **116**, 278 (1997).
[13]M. Alatalo, H. Kauppinen, K. Saarinen, M. J. Puska, H. Makinen, P. Hautojarvi, and R. M. Nieminen, Phys. Rev. B **51**, 4176 (1995).
[14]T. Friessnegg, S. Madhukar, B. Nielsen, A. R. Moodenbaugh, S. Aggarwal, D. J. Keeble, E. H. Poindexter, P. Mascher, and R. Ramesh, Phys. Rev. B **59**, 13365 (1999).
[15]K. Süvegh, A. Domj'an, R. Tarsoly, and A. Vértes, J. Radioanal. Nucl. Chem. **211**, 255 (1996).
[16]A. S. Hamid, A. Uedono, T. Chikyow, K. Uwe, K. Mochizuki, and S.

Kawaminami, Phys. Status Solidi A **203**, 300 (2006).
[17]R. A. Mackie, S. Singh, J. Laverock, S. B. Dugdale, and D. J. Keeble, Phys. Rev. B **79**, 014102 (2009).
[18]E. Borońśki and R. M. Nieminen, Phys. Rev. B **34**, 3820 (1986).
[19]J. Arponen and E. Pajanne, Ann. Phys. **121**, 343 (1979).
[20]D. J. Keeble, S. Singh, R. A. Mackie, M. Morozov, S. McGuire, and D. Damjanovic, Phys. Rev. B **76**, 144109 (2007).
[21]T. Torsti, M. Heiskanen, M. J. Puska, and R. M. Nieminen, MIKA: a multigrid-based program package for electronic structure calculations.
[22]P. Kirkegaard, N. J. Pedersen, and M. Eldrup, *PATFIT88: A Data-Processing System for Positron Annihilation Spectra on Mainframe and Personal Computers* (Risφ National Laboratory, Denmark, 1989).
[23]S. Janaswamy, G. S. Murthy, E. D. Dias, and V. R. K. Murthy, Mater. Lett. **55**, 414 (2002).
[24]T. Kolodiazhnyi, G. Annino, A. Younker, P. Malysz, P. Mascher, and H. Haneda, J. Eur. Ceram. Soc. **26**, 1921 (2006).
[25]U. Lehmann and H. Mueller-Buschbaum, Z. Anorg. Allg. Chem. **481**, 7 (1981).
[26]C.-T. Lee, Y.-C. Lin, C.-Y. Huang, C.-Y. Su, and C.-L. Hu, J. Am. Ceram. Soc. **90**, 483 (2007).
[27]Y. Dai, G. Zhao, and H. Liu, J. Appl. Phys. **105**, 034111 (2009).
[28]C.-T. Chia, Y.-C. Chen, H.-F. Cheng, and I.-N. Lin, J. Appl. Phys. **94**, 3360 (2003).
[29]S. J. Webb, J. Breeze, R. I. Scott, D. S. Cannell, D. M. Iddles, and N. M. Alford, J. Am. Ceram. Soc. **85**, 1753 (2002).
[30]D. Grebennikov and P. Mascher, J. Mater. Res. (submitted).
[31]M. P. Harmer, J. Chen, P. Peng, H. M. Chan, and D. M. Smyth, Ferroelectrics **97**, 263 (1989).
[32]J. Chen, H. M. Chan, and M. P. Harmer, J. Am. Ceram. Soc. **72**, 593 (1989).
[33]M. Wang, C. C. Cheng, C. D. Beling, S. Fung, and K. J. Chen, Phys. Status Solidi A **207**, 1332 (2010).
[34]T. A. Vanderah, T. R. Collins, W. Wong-Ng, R. S. Roth, and L. Farber, J. Alloys Compd. **346**, 116 (2002).
[35]S. Pagola, G. Polla, G. Leyva, M. T. Casais, J. A. Alonso, I. Rasines, and R. E. Carbonio, Mater. Sci. Forum **228-231**, 819 (1996).
[36]D. J. Barber, K. M. Moulding, J. I. Zhou, and M. Li, J. Mater. Sci. **32**, 1531 (1997).
[37]P. M. Mallinson, M. M. B. Allix, J. B. Claridge, R. M. Ibberson, D. M. Iddles, T. Price, and M. J. Rosseinsky, Angew. Chem. **44**, 7733 (2005).
[38]J. B. Goodenough, *Solid State Chemistry* (Marcel Dekker, New York, 1974).